

Electrochemical Impedance Spectroscopy Study for Cathodic Disbonding Test Technology on Three Layer Polyethylene Anticorrosive Coating under Full Immersion and Alternating Dry–Wet Environments

*Yingchun Chen, Xinhua Wang**, Yingchao Li, Gang Zheng, Xiyuan Tu

College of Mechanical Engineering and Applied Electronics Technology, Beijing University of Technology, Beijing, 100124, China

*E-mail: paper_bgdjd103@163.com

Received: 29 July 2016 / Accepted: 19 October 2016 / Published: 10 November 2016

Cathodic disbonding of three layer polyethylene (3LPE) anticorrosive coating under alternating dry–wet and full immersion environments is now a serious problem associated with oil and gas pipelines. In this study, under such specific environment, electrochemical impedance spectroscopy (EIS) technology was used to study the process and mechanism of cathodic disbanding behavior of broken 3LPE anticorrosive coating in 3.5% NaCl solution. The dry–wet cycle involved two steps of 12 h immersion followed by 12 h drying process. The results showed that broken 3LPE anticorrosive coating exhibited a starting potential of -1.28 V (vs. SCE) (-1.20 V (vs. CSE)) under full immersion environment. The impedance characteristic of broken 3LPE anticorrosive coating exposed to alternating dry–wet environment was similar to that under full immersion environment: the impedance of anticorrosive coating first increased and then decreased; however, the value of impedance under dry–wet process was significantly less than that under full immersion process. Dry–wet circulation significantly accelerated the corrosion reaction; moreover, anticorrosive coating failure rate was also significantly faster.

Keywords: Three layer polyethylene anticorrosive coating; Dry–wet alternate environment; Full immersion; Electrochemical impedance spectroscopy

1. INTRODUCTION

Global demand for energy is increasing significantly in order to fuel continued economic growth and industrialization. The oil and gas industry is one of the “pillar” industries that play a leading role in the national economy. Thus, oil and gas pipelines are playing an more important role

with the increasing demand for energy [1,2]. However, corrosion can weaken the structural integrity of a pipeline and make it unsafe for transportation of oil and gas. Therefore, anticorrosive coatings are principle tools for the extension of structural life of these pipelines. These coatings provide resistance to cathodic disbondment. Alternating dry–wet cycle is a common phenomenon in nature which significantly influences the protection provided by in service anticorrosive coating [1,2]. Serving in the marine environment, anticorrosive coating/metal system is often influenced by alternating dry–wet cycles, and the corrosive particles in the coating metal interface area exhibits enrichment phenomenon to accelerate the corrosion of metal [3,4].

At present, less attention has been paid to the research on cathodic disbonding of broken anticorrosive coating under dry–wet circulation. Li et al. studied the cathodic disbonding under the immersing and dry–wet cyclic conditions [5], and found that the process of cathode disbonding can be divided into three main stages. And they also discussed the base metal corrosion mechanism and how dry–wet circulation accelerated the degradation of anticorrosive coating. Electrochemical impedance spectroscopy (EIS) and Fourier transform infrared (FTIR) spectroscopy along with other methods were used by Qu et al. [6] to study the thick epoxy primer under full immersion and dry–wet alternate environment in 3.5% NaCl solution to understand the similarities and differences in anticorrosive coating failure process between two types of environments (full immersion and dry–wet alternate). Moreover, Wang et al. [7–10] have devoted extensive research efforts to the study of corrosion of pipelines. Most of the studies done on this topic focused mainly on organic anticorrosive coating; however, very few attentions have been paid to the broken three layer polyethylene (3LPE) anticorrosive coating cathodes under full immersion and dry–wet alternate environments.

Focusing on the failure of broken 3LPE anticorrosive coating on oil and gas pipelines under full immersion and alternating dry–wet environment, in this study, an alternate test device and full immersion test device were designed and developed under the initial potential of cathodic disbonding. Furthermore, degradation of 3LPE coating/pipeline steel under two different conditions was compared through EIS characteristics.

2. TEST CONTENT

2.1. Test materials and solution

Q235 steel pipeline coated with 3LPE anticorrosive coating was used as test material during the experiment.

The bottom layer of 3LPE anticorrosive coating consists of a high performance fusion bonded epoxy (FBE) resin powder comprising high molecular weight bisphenol A type epoxy resin which acts as a curing agent containing phenol hydroxyl resin, fillers, and additives. FBE forms a continuous film, directly bonded outside the pipe surface, and provides high adhesion and good cathodic disbonding resistance.

The middle tier of 3LPE anticorrosive coating consists of polyolefin adhesive with branch function. Polyolefin adhesive can adhere well with epoxy resin which is able to resist soil movement and temperature change caused by shear force.

High density modified polyethylene coating with carbon black as an antioxidant along with other additives is present on the outer surface of 3LPE anticorrosive coating, which acts as an excellent barrier against moisture. It provides durable strength and protects the adhesive layer. The underlying epoxy resin has strong ability to resist mechanical damage and reduce the possibility of stripping. Cathodic protection current is low to adapt the temperature range. Complete process of 3LPE coating is shown in Fig. 1.

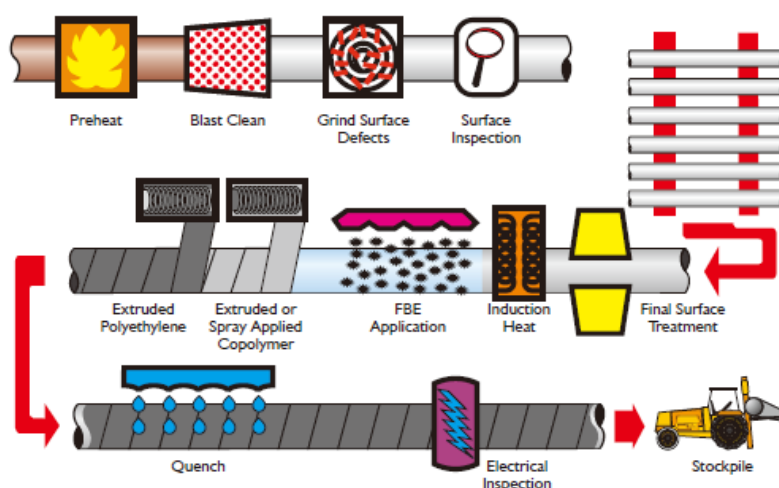


Figure 1. Process of coating oil and gas pipelines with 3LPE anticorrosive coating

Based on standard GB/T23257-2009 (polyethylene anticorrosive coating for buried steel pipeline), a $\Phi 6.4$ mm deep hole at coating surface (through anticorrosive layer) was artificially made, and the test medium was 3.5% NaCl solution.

2.2. Test method

Herein, we investigated the initial potential of cathodic disbonding for a broken hole of 3LPE coating in 3.5% NaCl solution. The cathodic disbonding test apparatus consisted of an electrolytic cell, potentiostat, and voltage meter. The testing temperature was set at room temperature. The function of the potentiostat and voltage meter is to provide a certain cathode potential that can be used to observe the anticorrosive layer stripping status within a certain time.

To observe the failure process of the anticorrosive coating caused by initial potential of cathodic disbonding under the immersion and alternating dry–wet cyclic conditions, dry–wet alternate test device and full immersion test device were built. A complete cycle for dry–wet alternate was 24 h (12 h immersion period followed by a 12 h drying period at room temperature), and an EIS test was

carried out after every 12 h. However, for full immersion, EIS test was carried out every 24 h on the sample.

2.3. Electrochemical impedance spectroscopy test

All electrochemical experiments were performed with PARSTAT 2273 advanced electrochemical workstation equipped with EIS testing instrument and measurement software PowerSuite. A standard three electrode system was used for all electrochemical experiments. Saturated calomel electrode (SCE) and platinum electrodes were used as reference and auxiliary electrodes, respectively. The study was performed with broken hole of 3 LPE coating/Q235 pipeline steel specimens with an effective area of 32.1536 cm². The test medium contained 3.5% NaCl solution. EIS scanning device with a frequency range of 10⁵–10⁻² Hz was employed. An AC sine wave of 10 mV amplitude was applied. During process of immersion, the composition of solution changes due to influence of corrosion and moisture evaporation; therefore, a regular replacement of the solution is required to reduce the effect of unnecessary factors.

3. RESULTS AND DISCUSSION

3.1. Effect of cathode potential on the disbonding of 3LPE anticorrosive coating

Disbonding condition of the hole in the sample was studied for 7 d as a cycle under different cathode potentials, i.e., -1.0, -1.5, -2, -2.5, -3.0, and -3.5 V [11].

The range of brown rust around the hole in the sample was observed and measured to decide the circle for stripping range on 3LPE anticorrosive coating. The circle associated with stripping of coating can be calculated by using the following equation (1):

$$D = \frac{\Delta d}{2} = \frac{d_2 - d_1}{2} \quad (1)$$

Where D is the stripping distance in mm; d_1 is diameter of the hole in the sample before test in mm; and d_2 is rust circle diameter after the test in mm.

Fig. 2 demonstrates that the disbonding distance is inversely proportional to the cathode potential. For the cathode potential greater than -1.5 V (vs. SCE), the corrosion layer does not exhibit disbonding phenomenon. However, if the potential is less than -1.5 V, the cathode disbonding distance decreases with the gradual increase in the potential. Therefore, the starting voltage for disbanding of anticorrosive coating is between -1.0 and -1.5 V; however, the Cathodic Protection Criterion indicates that the cathodic protection potential is around -0.85 to -1.5 V (vs. CSE). When potential reaches -1.5 V, anticorrosive coating shows obvious cathodic disbonding. Therefore, to obtain more accurate values, the initial potential of cathodic disbonding in a certain damage hole in the 3LPE anticorrosive coating sample is conducive to acquire Cathodic Protection Criteria.

Test similar to the above mentioned process was conducted, observing the disbonding distance under -1.20, -1.25, -1.28, and -1.30 V (vs. SCE), and the corresponding results are shown in Fig. 3.

No detachment is shown for a potential greater than -1.28 V (vs. SCE). In contrast, when the potential falls down to the value of -1.28 V (vs. SCE), disbonding of the anticorrosive coating starts and increases against the cathodic disbonding distance. These results can be explained as follows: when the cathode potential is less than -1.28 V, the negative cathode potential leads to the evolution of a hydrogen substrate beneath the anticorrosive coating that accelerates the disbonding failure of anticorrosive coating. As a result, the initial potential of 3LPE coating cathodes is -1.28 V (vs. SCE).

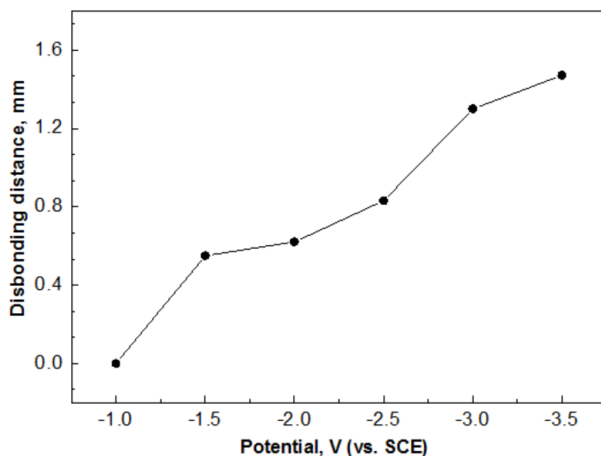


Figure 2. 3LPE disbonding distance with the change in cathode potential

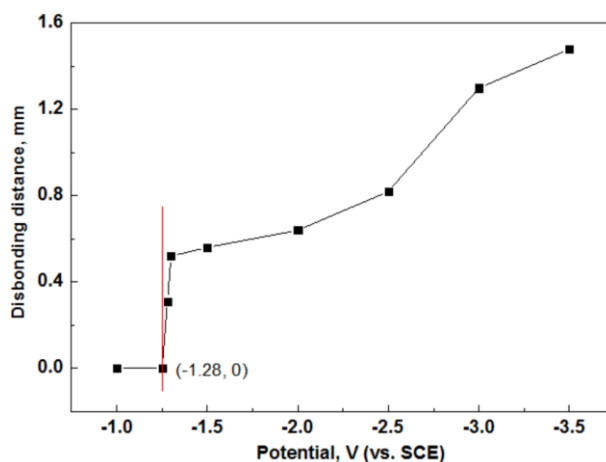


Figure 3. Effects of cathodic protection on 3 LPE coating

3.2. Electrochemical impedance spectrogram of anticorrosive coating exposed to full immersion under the initial potential of cathodic disbonding

EIS curves exhibiting the effect of cathode potential on 3LPE anticorrosive coating in 3.5% NaCl solution are shown in Fig. 4. The capacitive reactance arc shrinks with increase in immersion time. At the same time, due to the existence of broken hole in the sample, the Nyquist diagram with

low frequency band during immersion shows a double capacitive reactance arc characterized by two time constant features [17,18].

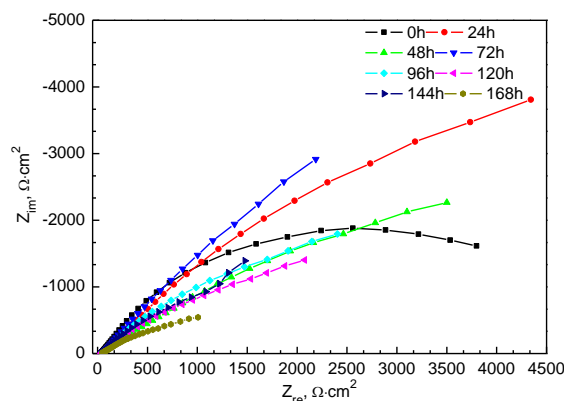


Figure 4. Nyquist spectrum of the anticorrosive coating under full immersion process

The matrix metal corrosion electrochemical reaction can start earlier due to the presence of corrosion medium at the metal/coating interface. Corresponding equivalent circuit model (EEC) for the process of immersion time of 0–72 h is shown in Fig. 5, based on the theoretical analysis [12–14]. With passage of time during the oxygen reduction reaction (as shown in equations (2)–(4)) [15,16], oxygen is dissolved and the surface of the electrode is consumed rapidly. The cathodic reaction is not enough to sustain stroke lesions of the anodic reaction; therefore, oxygen concentrations become the reaction steps of controlling which leads to the Warburg impedance diffusion tail by the EEC as shown in Fig. 6.

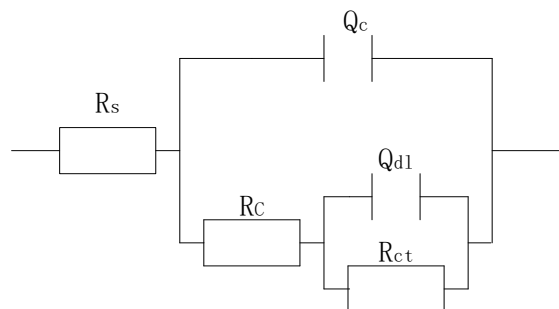


Figure 5. Equivalent circuit for full immersion 0–72 h

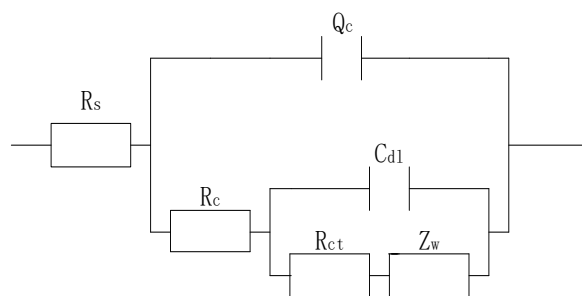


Figure 6. Equivalent circuit for full immersion 96–168 h

Where R_s is solution resistance; R_c is anticorrosive layer resistance; Q_c is anticorrosive layer capacitance; Q_{cdl} and R_{ct} represent the total damage at the bottom of the hole in the metal/solution interface double-layer capacitance and total charge transfer resistance, respectively; and Z_w represents the Warburg impedance.



Low frequency impedance modulus values can be used to evaluate the corrosion resistant coating performance. The changing trend of 3LPE anticorrosive coating sample's $|Z|_{0.1Hz}$ in 3.5% NaCl solution after full immersion is shown in Fig. 7.

The changing trend of anticorrosive layer can be divided into two stages, and the first phase involves the immersion for 0–24 h. During this period the anticorrosive coating impedance increases at early immersion. Thus, due to existence of broken anticorrosive coating, electrostatic shielding effect and higher IR voltage drop on the coating effect are decreased, which makes the coating matrix under the real protection potential close to the cathodic protection potential of -1.28 V (vs. SCE). At this stage the coating shows protective effect to some extent. The second stage initializes after 24 h due to the accumulation of corrosion products and generation of OH^- by the oxygen reduction reaction, thus resulting in alkaline environment and decrease in the impedance of the anticorrosive coating. After 168 h of immersion, when the impedance descends to $1162 \Omega \text{ cm}^2$, the anticorrosive coating loses the protection ability and disbonds with the sample.

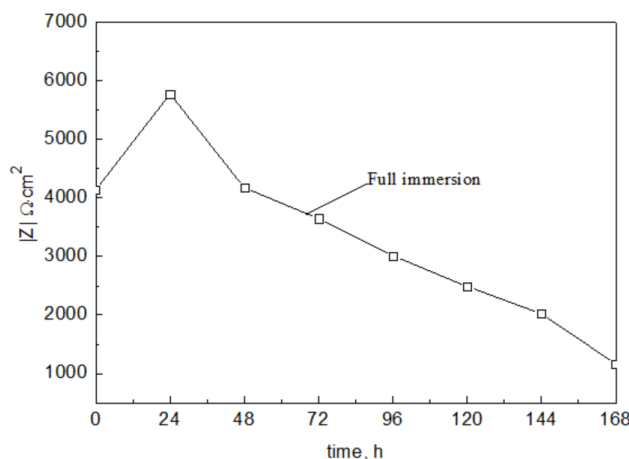


Figure 7. Impedance of anticorrosive coating in 3.5% NaCl solution ($f = 0.1$ Hz)

3.3. Electrochemical impedance spectroscopy of the anticorrosive coating under dry–wet alternate condition when the cathodic protection potential is -1.28 V (vs. SCE)

The EIS response of broken coating failure under the condition of dry–wet circulation process is shown in Fig. 8. Clearly, impedance spectra obviously change within two stage characteristics. During 0–36 h, due to the effective prevention of the corrosion of the metal matrix affected by the cathodic protection potential, the capacitive reactance arc radius becomes larger. Moreover, the

reactance arc radius decreases with extension of time. Throughout the immersion cycle, Nyquist diagrams were presented at low frequency double capacitive reactance arc due to the effect of broken hole, which was characterized by two time constant characteristics. Results of immersion during 0–36 h (EEC) are shown in Fig. 5. With the increasing time (60–108 h), the Warburg impedance appears, as shown in Fig. 6. With sustained dry–wet circulation, anticorrosive coating protection gradually disappears; the solution resistance R_s , anticorrosive coating resistance R_c , and interface reaction resistance R_{ct} are shown in a series in Fig. 10.

Fig. 9 shows anticorrosive coating impedance changes during the process of dry–wet cycle. As already know, corrosion products change lightly at the cathodic polarization potential [17,18]. Throughout the first and second stages of the process, impedance of anticorrosive coating exhibits an increasing tendency. This could be attributed to following phenomenon: the immersion corrosion products spread out into the affected area along with electrolyte solution during the process of drying, thus instigating the coating resistance to increase. Further, the matrix corrosion reaction begins to occur as the anticorrosive coating enters again into the wetting state. Thus the corrosion products again spread into the lesions triggering the coating resistance to increase gradually. With continuous dry–wet circulation, the impedance falls down more rapidly, which proves that the impedance falling speed during dry–wet circulation is faster than that under the full immersion condition [19–21].

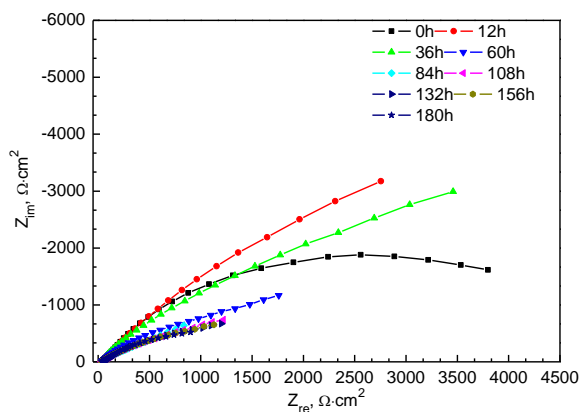


Figure 8. Nyquist spectrum of anticorrosive coating during the process of dry–wet circulation

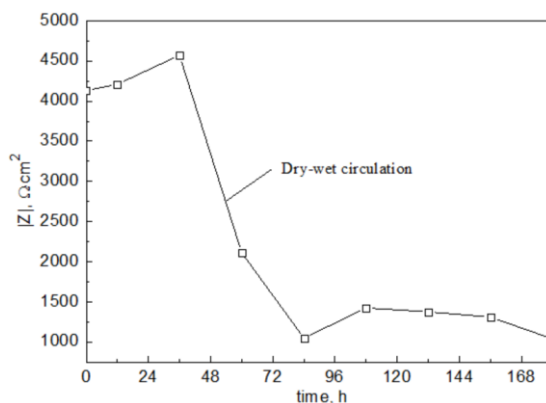


Figure 9. Impedance of anticorrosive coating under dry–wet circulation ($f = 0.1$ Hz)

This result demonstrates that the coating failure rate under dry–wet circulation condition is significantly faster than the failure rate under immersion environment because dry–wet circulation accelerated the failure of anticorrosive coating [9,10]. During the drying process, the disbanding speed of anticorrosive coating under dry–wet circulation is faster than that within full immersion due to the acceleration of oxygen reduction reaction, and the base metal corrosion for the sample under dry–wet circulation occurs rapidly. Therefore, fall of impedance under dry–wet circulation is larger than that during immersion process [22].

3.4. R_{ct} electrochemical parameters change over time

R_{ct} indicates the difficulty of charge across the electrodes and the electrolyte solution of the two phase interface during the process of the electrode reaction, when the potential is E [23,24]. EIS of immersion and dry–wet circulation processes can be achieved based on the equivalent circuits, and the changing trend of electrochemical parameters R_{ct} as shown in Fig. 11. Clearly, R_{ct} under dry–wet circulation process is smaller than that under the immersion process; and within 24–72 h, the decrease in amplitude of R_{ct} under dry–wet circulation is smaller than that during immersion process. Thus, the results illustrated that dry–wet alternate circulation environment was more unsuitable for anticorrosive coating as coating failure rate was significantly more under cathodic protection potential. Within 96–180 h of dry–wet alternate condition, R_{ct} generally remains stable and displays a slowdown trend. This indicates that the corrosion rate of matrix slows down after 96 h. This is attributed to the interface effect generated by the corrosion products which makes the matrix to slow down the corrosion development. Compared to immersion process, under dry–wet circulation, electrochemical reaction rate of matrix under anticorrosive coating is much faster. This is because in dry conditions, the flow of oxygen is directed into the broken holes through the process of diffusion. Thus, during soaking process, oxygen reduction reaction continues which makes the cathodic protection potential insufficient to reach the protection potential, and therefore unable to realize the protection of substrate, thus it accelerates the corrosion of the base. Possibly, during the process of drying, Cl^- ions in the solution gather in the broken hole and anticorrosive layer gaps which results in increase in the concentration of Cl^- ions. This phenomenon accelerates the corrosion of substrate and coating failure. Moreover, gaps between the coating and substrate gradually increases and forms a solution in the coating/substrate interface channel due to the repeated occurrence of water absorption and dehydration swelling and shrinkage during the process, thus leading to the acceleration of the failure of the coating.

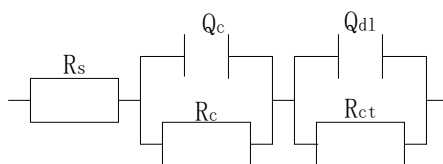


Figure 10. Equivalent circuit during the process of dry–wet cycles between 108–180 h

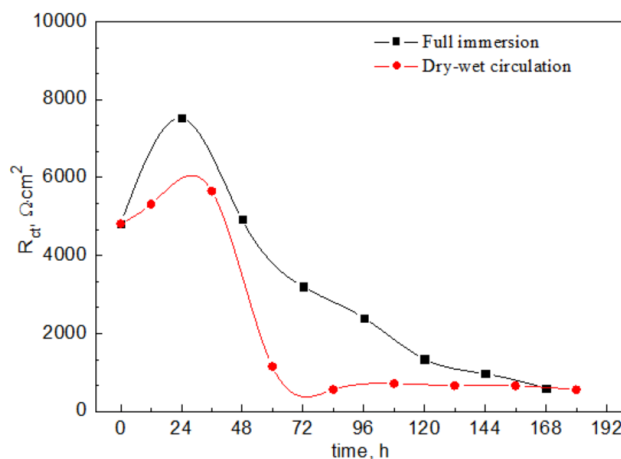


Figure 11. R_{ct} during immersion and under dry–wet cyclic conditions

4. CONCLUSION

(1) The disbonding distance of anticorrosive coating increased with the loss of the cathode potential, 3LPE coating cathodes starting voltage was found to be -1.28 V (vs. SCE); therefore, the best protective potential of 3 LPE coating is in the range -0.85 to -1.28 V (vs. SCE).

(2) Under the initial potential of cathodic disbonding of 3LPE anticorrosive coating, the changing behavior of impedance in the dry–wet circulation environment was found to be similar to that in the full immersion process, and the impedance of anticorrosive coating first increased and then decreased. The value of impedance within dry–wet circulation was much smaller than that in full immersion process; therefore, dry–wet circulation significantly accelerated the corrosion reaction, and anticorrosive layer failure rate was significantly faster.

(3) During 24–72 h, dry–wet circulation immersion coating of R_{ct} was smaller than a single immersion process, the R_{ct} values decrease range was higher than that of immersion process. This study indicates that under the cathodic protection potential, compared to the single immersion, dry–wet alternate circulation environment was more destructive on the coating, and coating failure rate was also significantly higher.

ACKNOWLEDGEMENTS

This study is supported by National Natural Science Foundation of China (No. 51471011).

References

1. M. Hudson, PhD thesis, Cranfield University, UK (2004).
2. F. Mohammadi, F. F. Eliyan, Akram Alfantazi, *Corros. Sci.*, 63 (2012) 323.
3. Y. Chen, S. Zhang S, D. Yu, W. Wang, M. Xiong, *Measurement*, 65(2015) 227-232.
4. Y. Chen, S. Zhang S, Wang, M. Xiong, Proceedings of the Institution of Mechanical Engineers Part M Journal of Engineering for the Maritime Environment, 2014.
5. Y. Li, J. Wang, W. Zhang, *Electrochemistry*, 16(2010) 393-400.

6. S. Qu, X. Zhao, J. Tang, Y. Zuo, *Corrosion and Protection*, 34(2013) 137-141.
7. X. Wang, X. Tang X, L. Wang, C. Wang, W. Zhou, *Journal of Natural Gas Science & Engineering*, 21(2014) 474-480.
8. X. Wang, X. Tang X, L. Wang, Z. Guo, *International Journal of Electrochemical Science*, 9(2014) 4574-4588.
9. X. Wang, C. Wang, X. Tang, Z. Guo, *International Journal of Electrochemical Science*, 9(2014) 8199-8210.
10. X. Wang, C. Wang, X. Tang, Z. Guo, *International Journal of Electrochemical Science*, 9(2014) 7660-7671.
11. T. Tsuru, *Boshoku Gijutsu*, 34 (1985) 36.
12. Z. L. Li, Q. M. Ding, Y.F. Zhang, J. J. Li, S. L. Li, *Corrosion & Protection*, 31 (2010) 436.
13. F. Mansfeld, *Russ. J. Electrochem.*, 36 (2000) 1205.
14. C. N. Cao, J. Q. Zhang, *An introduction to electrochemical impedance spectroscopy*, Beijing: Science Press., 2002.
15. T. Tsuru, *Bosei Kanri*, 30 (1986) 1.
16. G. H. Zhang, M. Gong, Q. Tang, T. Zhang, X. M. Zeng, *Corrosion & Protection*, 32 (2011) 868.
17. M. C. Bernard, S. Joiret, A. Hugot Le Goff, *Russ. J. Electrochem.*, 40 (2004) 235.
18. M. C. Li, H. C. Lin, C. N. Cao, *Journal of Chinese Society for Corrosion and Protection*, 20 (2000) 111.
19. R. P. V. Cruz, A. Nishikata, T. Tsuru, *Corros. Sci*, 38(1996) 1397-1406.
20. B. Panda, R. Balasubramaniam, G. Dwivedi, *Corros. Sci*, 50(2008) 1684-1692.
21. G. Elliott, *Journal of Applied Electrochemistry*, 35(2005) 347-353.
22. A. P. Yadav, A. Nishikata, T. Tsuru. *Corros. Sci*, 46(2004) 169-181.
23. U. Rammelt, G. Reinhard, *Prog. Org. Coat*, 21(1992) 205.
24. J. R. Vilche, E. C. Bucharsy, C. A. Giudice, *Corros. Sci*, 44(2002) 1287-1309.